

# The Kagomé Topology of the Gallium and Indium Metal-Organic Framework Types with a MIL-68 Structure: Synthesis, XRD, Solid-State NMR Characterizations, and Hydrogen Adsorption

Christophe Volklinger,<sup>†</sup> Mohamed Meddouri,<sup>†</sup> Thierry Loiseau,<sup>\*,†</sup> Nathalie Guillou,<sup>†</sup> Jérôme Marrot,<sup>†</sup> Gérard Férey,<sup>†,‡</sup> Mohamed Haouas,<sup>§</sup> Francis Taulelle,<sup>§</sup> Nathalie Audebrand,<sup>||</sup> and Michel Latroche<sup>⊥</sup>

*Institut Lavoisier (UMR CNRS 8180), Porous Solids Group, Université de Versailles Saint Quentin en Yvelines, 45, Avenue des Etats-Unis, 78035 Versailles, France, Institut Universitaire de France, Institut Lavoisier (UMR CNRS 8180), Tectospin Group, Université de Versailles Saint Quentin en Yvelines, 45, Avenue des Etats-Unis, 78035 Versailles, France, Sciences Chimiques de Rennes (UMR CNRS 6226), Université de Rennes 1, 263, Avenue du Général Leclerc, 35042 Rennes, France, and ICMPE-CMTR (UMR CNRS 7182), 2-8, Rue Henri Dunant, 94320 Thiais, France*

Received August 28, 2008

The vanadium-based terephthalate analogs of MIL-68 have been obtained with gallium and indium (network composition:  $M(\text{OH})(\text{O}_2\text{C}-\text{C}_6\text{H}_4-\text{CO}_2)$ ,  $M = \text{Ga}$  or  $\text{In}$ ) by using a solvothermal synthesis technique using *N,N*-dimethylformamide as a solvent (10 and 48 h, for Ga and In, respectively, at 100 °C). They have been characterized by X-ray diffraction analysis; vibrational spectroscopy; and solid-state  $^1\text{H}$  and  $^1\text{H}-^1\text{H}$  radio-frequency-driven dipolar recoupling (RFDR),  $^1\text{H}-^1\text{H}$  double quantum correlation (DQ), and  $^{13}\text{C}\{^1\text{H}\}$  cross polarization magic angle spinning (CPMAS) NMR spectroscopy. The three-dimensional network with a Kagomé-like lattice is built up from the connection of infinite trans-connected chains of octahedral units  $\text{MO}_4(\text{OH})_2$  ( $M = \text{Ga}$  or  $\text{In}$ ), linked to each other through the terephthalate ligands in order to generate triangular and hexagonal one-dimensional channels. The presence of DMF molecules with strong interactions within the channels as well as their departure upon calcination (150 °C under a primary vacuum) of the materials has been confirmed by subjecting MIL-68 (Ga) to solid-state  $^1\text{H}$  MAS NMR. The  $^1\text{H}-^1\text{H}$  RFDR and  $^1\text{H}-^1\text{H}$  DQ spectra revealed important information on the spatial arrangement of the guest species with respect to the hybrid organic–inorganic network.  $^{13}\text{C}\{^1\text{H}\}$  CPMAS NMR of activated samples provided crystallographically independent sites in agreement with X-ray diffraction structure determination. Brunauer–Emmett–Teller surface areas are 1117(24) and 746(31)  $\text{m}^2 \text{g}^{-1}$  for MIL-98 (Ga) and MIL-68 (In), respectively. Hydrogen adsorption isotherms have been measured at 77 K, and the storage capacities are found to be 2.46 and 1.98 wt % under a saturated pressure of 4 MPa for MIL-68 (Ga) and MIL-68 (In), respectively. For comparison, the hydrogen uptake for the aluminum trimesate MIL-110, which has an open framework with 16 Å channels, is 3 wt % under 4 MPa.

## Introduction

In the past decade, the search of new crystalline hybrid materials with infinite three-dimensional networks involving

the combination of inorganic building units with organic ligands has grown exponentially. This novel class of solids, named coordination polymers or metal-organic frameworks (MOFs),<sup>1–3</sup> exhibits complex structural topologies with significant porous properties and large aperture windows (greater than those observed in zeolites), which can be used

\* Author to whom correspondence should be addressed. Phone: (33) 1 39 254 373. Fax: (33) 1 39 254 358. E-mail: loiseau@chimie.uvsq.fr.

<sup>†</sup> Porous Solids Group, Université de Versailles Saint Quentin en Yvelines.

<sup>‡</sup> Institut Universitaire de France.

<sup>§</sup> Tectospin Group, Université de Versailles Saint Quentin en Yvelines.

<sup>||</sup> Université de Rennes 1.

<sup>⊥</sup> ICMPE-CMTR (UMR CNRS 7182).

(1) Férey, G. *Chem. Soc. Rev.* **2008**, *37*, 191.

(2) Yaghi, O. M.; O'Keeffe, M.; Ockwig, N. W.; Chae, H. K.; Eddaoudi, M.; Kim, J. *Nature* **2003**, *423*, 705.

(3) Kitagawa, S.; Kitaura, R.; Noro, S.-I. *Angew. Chem., Int. Ed.* **2004**, *43*, 2334.

for different applications such as gas storage, separation, catalysis,<sup>4,5</sup> magnetism,<sup>6</sup> drug release,<sup>7</sup> and so forth. These compounds are prepared from metallic atoms, which may condense via oxo or hydroxo bridgings to form discrete or infinite inorganic motifs connected to rigid organic molecules containing benzene rings (usually aromatic carboxylates) in order to get robust open frameworks with delimited sizes of cavities or channels. A large effort has been devoted to the study of the reactivity of the first row of divalent transition metals (e.g., Cu<sup>2+</sup>, Zn<sup>2+</sup>), but fewer works have reported the synthesis of MOF-type compounds incorporating trivalent metals, especially for the p elements of the periodic table such as aluminum, gallium, or indium. For instance, in Versailles, we described the formation of several open-framework carboxylates (MIL-*n*, for Materials Institut Lavoisier) containing aluminum (MIL-53,<sup>8</sup> MIL-69,<sup>9</sup> MIL-96,<sup>10</sup> and MIL-110<sup>11</sup>), gallium (MIL-61<sup>12</sup> and MIL-96<sup>13</sup>), or indium (MIL-96,<sup>14</sup> MIL-60,<sup>15</sup> and MIL-119<sup>15</sup>). Furthermore, the syntheses of indium carboxylates have been extensively investigated by other groups,<sup>16–27</sup> and different topologies have already been reported. Some of them are identical to

other previous networks observed with trivalent transition metals such as vanadium (MIL-59<sup>24,28</sup> and MIL-61<sup>18,29</sup>) or chromium (MIL-53<sup>21,30</sup>).

This contribution deals with the solvothermal synthesis and structural characterization of the analogs of the vanadium-based terephthalate MIL-68,<sup>31</sup> V(OH)(O<sub>2</sub>C–C<sub>6</sub>H<sub>4</sub>–CO<sub>2</sub>), obtained with gallium and indium (abbreviated as MIL-68 (Ga) and MIL-68 (In)). Its three-dimensional network is an illustration of a Kagomé-like lattice<sup>32,33</sup> with infinite chains of octahedral units linked through the terephthalate ligand, delimiting triangular and hexagonal channels (window diameter 16 Å). The structures of both compounds are analyzed by X-ray diffraction. Solid-state NMR spectroscopy (<sup>1</sup>H, <sup>13</sup>C) was used in order to shed light on the crystal symmetry of the MIL-68 network as well as the location of the trapped species (H<sub>2</sub>O, DMF) within the channels. The evacuation procedure of these encapsulated molecules was monitored by NMR, and the activated samples have been characterized by the Brunauer–Emmett–Teller (BET) method. Their surface area estimations were 1117(24) (Ga) and 746(31) m<sup>2</sup> g<sup>−1</sup> (In). The Langmuir surface areas were found to be 1410(2) (Ga) and 1139(5) m<sup>2</sup> g<sup>−1</sup> (In). Hydrogen adsorption isotherms revealed uptakes of 2.46 wt % and 1.98 wt % for the gallium and indium phases, respectively. For comparison, the hydrogen uptake was also measured on the aluminum trimesate MIL-110<sup>11</sup> with an organic–inorganic framework containing 16 Å channels.

## Experimental Section

**Synthesis.** Both MIL-68 (In) and MIL-68 (Ga) phases were obtained by using solvothermal treatment involving N,N-dimethylformamide (DMF) as the main solvent. Starting reactants are gallium nitrate (Ga(NO<sub>3</sub>)<sub>3</sub>·xH<sub>2</sub>O, Alfa Aesar, 99.9%), indium nitrate (In(NO<sub>3</sub>)<sub>3</sub>·5H<sub>2</sub>O, Alfa Aesar, 99.9%), terephthalic acid (HO<sub>2</sub>C–C<sub>6</sub>H<sub>4</sub>–CO<sub>2</sub>H, Aldrich, 98%, abbreviated as bdcH<sub>2</sub>), and N,N-dimethylformamide ((CH<sub>3</sub>)<sub>2</sub>NCHO, Fluka, > 99.9%).

**MIL-68 (In).** The indium analog of MIL-68 was prepared from a mixture of indium nitrate (1.05 mmol, 408.2 mg), terephthalic acid (1.2 mmol, 200 mg), and DMF (70 mmol, 5 mL). The reactants were placed in a Teflon-lined Parr autoclave and heated for 48 h at 100 °C in an oven. The resulting white powder was filtered off and washed with DMF and consisted of elongated needlelike crystallites of 20–200 μm size (Figure 1). The yield was 83% based on indium. Elemental analysis gave the following: In, 26.15%; N, 3.45%; and C, 30.4%. This corresponds to the following chemical formula for MIL-68 (In): In(OH)(O<sub>2</sub>C–C<sub>6</sub>H<sub>4</sub>–CO<sub>2</sub>)·1.0 DMF·zH<sub>2</sub>O. In a more diluted solution (0.75 mmol In/0.9 mmol bdcH<sub>2</sub>/70 mmol DMF), a second phase appeared with typical elongated hexagonal prismatic crystals (quartzlike shape) and was found to correspond to the indium terephthalate QMOF-2 (InH(O<sub>2</sub>C–C<sub>6</sub>H<sub>4</sub>–CO<sub>2</sub>)<sub>2</sub>), previously described by Sun et al.<sup>17</sup> In water, the layerlike In<sub>2</sub>(OH)<sub>3</sub>(O<sub>2</sub>C–C<sub>6</sub>H<sub>4</sub>–CO<sub>2</sub>)<sub>1.5</sub><sup>16</sup> or the channel-based

- (4) Janiak, C. *Dalton Trans.* **2003**, 14, 2781.
- (5) Mueller, U.; Schubert, M.; Teich, F.; Puetter, H.; Schierle-Arndt, K.; Pastré, J. *J. Mater. Chem.* **2006**, 16, 626.
- (6) Maspoch, D.; Ruiz-Molina, D.; Veciana, J. *Chem. Soc. Rev.* **2007**, 36, 770.
- (7) Horcajada, P.; Serre, C.; Vallet-Regi, M.; Sebban, M.; Taulelle, F.; Férey, G. *Angew. Chem., Int. Ed.* **2006**, 45, 5974.
- (8) Loiseau, T.; Serre, C.; Huguenard, C.; Fink, G.; Taulelle, F.; Henry, M.; Bataille, T.; Férey, G. *Chem.—Eur. J.* **2004**, 10, 1373.
- (9) Loiseau, T.; Mellot-Draznieks, C.; Muguerra, H.; Férey, G.; Haouas, M.; Taulelle, F. *C. R. Chim.* **2005**, 8, 765.
- (10) Loiseau, T.; Lecroq, L.; Volklinger, C.; Marrot, J.; Férey, G.; Haouas, M.; Taulelle, F.; Bourrelly, S.; Llewellyn, P. L.; Latroche, M. *J. Am. Chem. Soc.* **2006**, 128, 10223.
- (11) Volklinger, C.; Popov, D.; Loiseau, T.; Guillou, N.; Férey, G.; Haouas, M.; Taulelle, F.; Mellot-Draznieks, C.; Burghammer, M.; Riekel, C. *Nat. Mater.* **2007**, 6, 760.
- (12) Loiseau, T.; Muguerra, H.; Haouas, M.; Taulelle, F.; Férey, G. *Solid State Sci.* **2005**, 7, 603.
- (13) Volklinger, C.; Loiseau, T.; Férey, G.; Morais, C.; Taulelle, F.; Montouillout, V.; Massiot, D. *Microporous Mesoporous Mater.* **2007**, 105, 111.
- (14) Volklinger, C.; Loiseau, T. *Mater. Res. Bull.* **2006**, 41, 948.
- (15) Volklinger, C.; Loiseau, T.; Férey, G. *Solid State Sci.* **2009**, 11, in press.
- (16) Gomez-Lor, B.; Gutierrez-Puebla, E.; Monge, M. A.; Ruiz-Valero, C.; Snejko, N. *Inorg. Chem.* **2002**, 41, 2429.
- (17) Sun, J. S.; Weng, L.; Zhou, Y.; Chen, J.; Chen, Z.; Liu, Z.; Zhao, D. *Ang. Chem., Int. Ed.* **2002**, 41, 4471.
- (18) Lin, Z.-Z.; Jiang, F.-L.; Chen, L.; Yuan, D.-Q.; Zhou, Y.-F.; Hong, M.-C. *Eur. J. Inorg. Chem.* **2005**, 77.
- (19) Lin, Z.-Z.; Jiang, F.-L.; Yuan, D.-Q.; Chen, L.; Zhou, Y.-F.; Hong, M.-C. *Eur. J. Inorg. Chem.* **2005**, 1927.
- (20) Lin, Z.; Jiang, F.; Chen, L.; Yuan, D.; Hong, M. *Inorg. Chem.* **2005**, 44, 73.
- (21) Anokhina, E. V.; Vougo-Zanda, M.; Wang, X.; Jacobson, A. J. *J. Am. Chem. Soc.* **2005**, 127, 15000.
- (22) Lin, Z.-Z.; Luo, J.-H.; Hong, M.-C.; Wang, R.-H.; Han, L.; Cao, R. *J. Solid State Chem.* **2004**, 177, 2494.
- (23) Wang, Y.-L.; Liu, Q.-Y.; Zhong, S.-L. *Acta Crystallogr., Sect. C* **2006**, 62, m395.
- (24) Liu, Y.; Eubank, J. F.; Cairns, A. J.; Eckert, J.; Kravtsov, V. C.; Luebke, R.; Eddaoudi, M. *Angew. Chem., Int. Ed.* **2007**, 46, 3278.
- (25) Vougo-Zanda, M.; Wang, X.; Jacobson, A. J. *Inorg. Chem.* **2007**, 46, 8819.
- (26) Gandara, F.; Gomez-Lor, B.; Gutierrez-Puebla, E.; Iglesias, M.; Monge, M. A.; Proserpio, D. M.; Snejko, N. *Chem. Mater.* **2008**, 20, 72.
- (27) Guo, Z.; Li, Y.; Yuan, W.; Zhu, X.; Li, X.; Cao, R. *Eur. J. Inorg. Chem.* **2008**, 1326.

- (28) Barthelet, K.; Riou, D.; Férey, G. *Chem. Commun.* **2002**, 1492.
- (29) Barthelet, K.; Riou, D.; Noguez, M.; Férey, G. *Inorg. Chem.* **2003**, 42, 1739.
- (30) Serre, C.; Millange, F.; Thouvenot, C.; Noguez, M.; Marsolier, G.; Louër, D.; Férey, G. *J. Am. Chem. Soc.* **2002**, 124, 13519.
- (31) Barthelet, K.; Marrot, J.; Férey, G.; Riou, D. *Chem. Commun.* **2004**, 520.
- (32) Syozi, I. *Prog. Theor. Phys.* **1951**, 6, 306.
- (33) Pati, S. K.; Rao, C. N. R. *Chem. Commun.* **2008**, 4683.

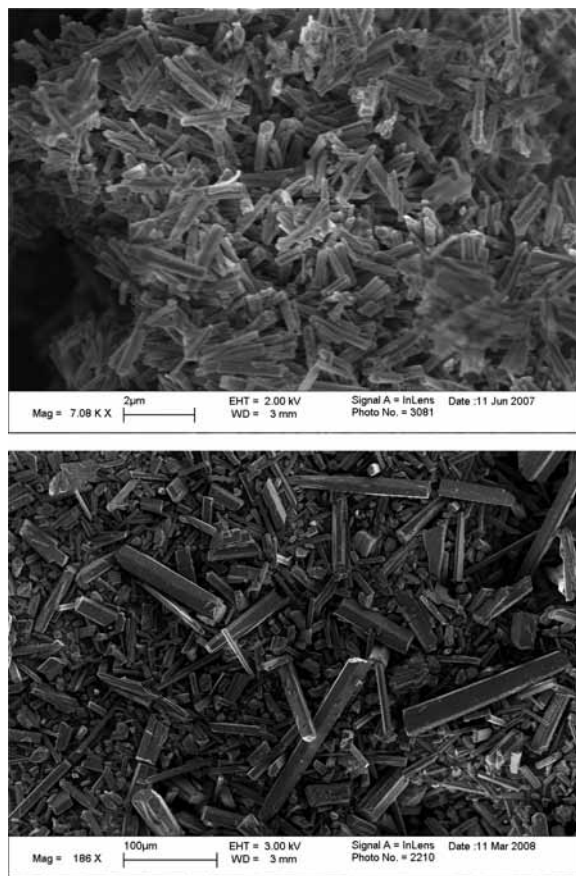


**Figure 1.** SEM photographs of the as-synthesized compounds (top) MIL-68 (Ga) and (bottom) MIL-68 (In), showing the needlelike crystals with different lengths (2–5  $\mu\text{m}$  for the Ga-based phase and 20–200  $\mu\text{m}$  for the In-based phase).

$\text{In}(\text{OH})(\text{O}_2\text{C}-\text{C}_6\text{H}_4-\text{CO}_2) \cdot 0.75(\text{O}_2\text{C}-\text{C}_6\text{H}_4-\text{CO}_2)^{21}$  indium terephthalates have been isolated.

**MIL-68 (Ga).** The gallium-based MIL-68 compound was synthesized from a mixture of gallium nitrate (0.8 mmol, 207.4 mg), terephthalic acid (0.6 mmol, 100 mg), and DMF (70 mmol, 5 mL). The reactants were placed in a Teflon-lined Parr autoclave and heated for 10 h at 100  $^\circ\text{C}$  in an oven. This resulted in the formation of a white powdered phase, which was filtered off and washed with DMF. The yield was 52% based on gallium. Elemental analysis gave the following: Ga, 18.14%; N, 3.0%; and C, 33.5%. This corresponds to the following chemical formula for MIL-68 (Ga):  $\text{Ga}(\text{OH})(\text{O}_2\text{C}-\text{C}_6\text{H}_4-\text{CO}_2) \cdot 0.9\text{DMF} \cdot z\text{H}_2\text{O}$ . Scanning electron microscopy shows that the MIL-68 (Ga) phase is composed of small needlelike crystallites of  $\approx 2 \mu\text{m}$  length (Figure 1). In water, the gallium analog of MIL-53<sup>34</sup> was formed, and details of the structural features will be discussed elsewhere.<sup>35</sup>

For both compounds, infrared spectra (using KBr pellet) show peaks at 2800 and 1660  $\text{cm}^{-1}$  corresponding to the vibrations of N–C and C=O bonds of the free DMF molecules. The adsorption bands of the C–O carboxyl bonds attached to the metal centers of the bdc ligand are visible at 1582 and 1573  $\text{cm}^{-1}$  for Ga and In, respectively. No free carboxylate species, corresponding to the range 1730–1680  $\text{cm}^{-1}$ , is observed.

In order to remove the organic species encapsulated within the pore of the open framework, both activated MIL-68 (Ga) and MIL-68 (In) phases were calcined overnight at 200  $^\circ\text{C}$  in a furnace. In ambient air, rehydration occurs. Thus, the activated samples were left in an inert atmosphere in order to prevent from any hydrolysis

reaction, which induces the decomposition of the structures after several weeks.

**Single-Crystal X-Ray Diffraction.** A colorless needlelike crystal of the indium-based MIL-68 (0.26  $\times$  0.04  $\times$  0.03 mm) was selected under a polarizing optical microscope and glued onto a glass fiber for a single-crystal X-ray diffraction experiment. X-ray intensity data were collected on a Bruker X8-APEX2 CCD area-detector diffractometer using Mo K $\alpha$  radiation ( $\lambda = 0.71073 \text{ \AA}$ ). Four sets of narrow data frames (60 s per frame) were collected at different values of  $\theta$  for two and two initial values of  $\phi$  and  $\omega$ , respectively, using 0.3 $^\circ$  increments of  $\phi$  or  $\omega$ . Data reduction was accomplished using SAINT V7.03. The substantial redundancy in data allowed a semiempirical absorption correction (SADABS V2.10) to be applied, on the basis of multiple measurements of equivalent reflections. The structure was solved by direct methods, developed by successive difference Fourier syntheses, and refined by full-matrix least squares on all  $F^2$  data using SHELXTL V6.12. The MIL-68 (In) crystal was first indexed in a hexagonal cell with the following parameters:  $a = 21.7584(4)$  and  $c = 7.2330(1) \text{ \AA}$  and  $V = 2965.53(9) \text{ \AA}^3$ . A structural model was found in  $P6_3/mmc$  (no. 194) with one crystallographically inequivalent indium atom (6g), two oxygen atoms (6h and 24l), and three carbon atoms (24l and  $2 \times 12j$ ). The final reliability factor converged to  $R_1 = 0.11$ , but abnormally large thermal displacement parameters ( $U \approx 0.3 \text{ \AA}^2$ ) were observed for the nonmetal atoms, such as oxygen and carbon atoms from the terephthalate moieties. This was not the case for the heaviest atoms, for which indium positions fit well with the hexagonal symmetry. The structure model was then considered in the parent orthorhombic symmetry with a double cell volume:  $a = 21.7739(6)$ ,  $b = 37.677(1)$ , and  $c = 7.2330(1) \text{ \AA}$  and  $V = 5933.8(2) \text{ \AA}^3$  in  $Cmcm$  (no. 63), as previously reported for the vanadium analog.<sup>31</sup> Hydrogen atoms were included in calculated positions and allowed to ride on their parent carbon atoms. Disordered N,N-dimethylformamide species were found to be trapped within only the small triangular channels of the structure. The corresponding carbon, oxygen, and nitrogen atoms have been refined with a fixed 50% occupancy. The final refinement including anisotropic thermal parameters of all non-hydrogen atoms converged to  $R_1 = 0.0527$  and  $wR^2 = 0.1900$ . The crystal data are given in Table 1 (atomic coordinates are in the Supporting Information).

**Powder X-Ray Diffraction Analysis.** In the absence of a suitable single crystal, the determination of the gallium analog of MIL-68 was carried out from X-ray powder diffraction data. In order to avoid Bragg reflection contributions of the trapped species within the channel of the structure, activated powdered MIL-68 (Ga) (heated overnight at 200  $^\circ\text{C}$  in a furnace) was introduced into a 0.5 mm glass capillary. The pattern was scanned at room temperature on a Bruker D8 Advance diffractometer with Debye–Scherrer geometry, in the range  $2\theta = 3\text{--}85^\circ$  with a step length of 0.015 $^\circ(2\theta)$  and a counting time of 290 s per step. The D8 system is equipped with a Ge(111) monochromator, producing Cu K $\alpha_1$  radiation ( $\lambda = 1.540598 \text{ \AA}$ ), and a Sol-X detector. Indexing and refinements were performed using the Topas software suite.<sup>36</sup> The hexagonal unit cell given above could not index all lines, and systematic extinctions of the  $P6_3/mmc$  space group were not consistent with the powder diffraction pattern. All lines were indexed in the orthorhombic symmetry with parameters similar to those of MIL-68 (In) (see Table 1), and a subsequent Pawley structure-independent fit to the

(34) Vougo-Zanda, M.; Huang, J.; Anokhina, E.; Wang, X.; Jacobson, A. J. *Inorg. Chem.* **2008**, *47*, [Online]

(35) Volkringer, C.; Loiseau, T.; Guillou, N.; Férey, G.; Audebrand, N.; Elkaim, E.; Vimont, A.; Daturi, M. *Manuscript in preparation*, 2009.

(36) *Topas V3.0*; Bruker AXS Ltd.: Madison, WI, 2004.

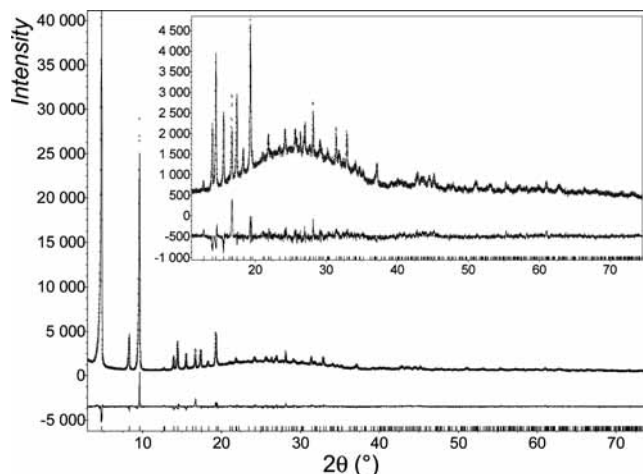


**Table 1.** Crystal Data and Structure Refinement for As-Synthesized MIL-68 (In) from Single-Crystal and Activated MIL-68 (Ga) from Powder

identification code	MIL-68 (In)	MIL-68 (Ga)
empirical formula	In <sub>3</sub> O <sub>15.5</sub> C <sub>25.5</sub> H <sub>12</sub> N <sub>0.5</sub>	Ga <sub>3</sub> O <sub>15</sub> C <sub>24</sub> H <sub>15</sub>
formula weight	917.82 g mol <sup>-1</sup>	752.52 g mol <sup>-1</sup>
temperature	293(2) K	293(2) K
wavelength	0.71073 Å	1.5405981 Å
crystal system, space group	orthorhombic, <i>Cmcm</i>	orthorhombic, <i>Cmcm</i>
unit cell dimensions	<i>a</i> = 21.7739(6) Å <i>b</i> = 37.677(1) Å <i>c</i> = 7.2330(1) Å	<i>a</i> = 21.176(4) Å <i>b</i> = 36.703(8) Å <i>c</i> = 6.7423(4) Å
volume	5933.8(2) Å <sup>3</sup>	5240(2) Å <sup>3</sup>
Z, calculated density	4, 1.027 g.cm <sup>-3</sup>	4, 0.954 g.cm <sup>-3</sup>
abs coeff	1.193 mm <sup>-1</sup>	
F(000)	1758	
crystal size	0.26 × 0.04 × 0.03 mm	
Θ range for data collection	1.08 to 30.06°	2.5 to 45°
limiting indices	-30 ≤ <i>h</i> ≤ 30, -53 ≤ <i>k</i> ≤ 53, -9 ≤ <i>l</i> ≤ 10	
reflns collected/unique	54894/4779 [R(int) = 0.0434]	811
completeness to Θ = 30.06	99.8%	
abs correction	semiempirical from equivalents	
refinement method	full-matrix least squares on F <sup>2</sup>	
data/restraints/params	4779/4/124	811/5/9
goodness-of-fit on F <sup>2</sup>	1.087	
final R indices [I > 2σ(I)]	R1 = 0.0527, wR2 = 0.1900	
R indices (all data)	R1 = 0.0762, wR2 = 0.2029	
Largest diff. peak and hole	3.820 and -3.789 e Å <sup>-3</sup>	
R <sub>wp</sub> /R <sub>Bragg</sub>		0.0573/0.0383

powder pattern confirmed the adequacy with the *Cmcm* space group. The atomic coordinates of the MIL-68 (In) skeleton were used as the starting model in the Rietveld refinement, and the two independent terephthalate anions were treated as rigid bodies. The first one centered on the 4*c* Wyckoff site was allowed to translate only along the *b* axis, whereas the second one centered on the 8*g* Wyckoff site was free to translate and rotate in two dimensions in the unit cell. At the final stage, Rietveld refinement involved the following parameters: three atomic coordinates, three translation and two rotation parameters of rigid bodies, one scale factor, one zero point, three cell parameters, 11 background parameters, and seven parameters to model the evolution of asymmetric diffraction line shape. Soft restraints were maintained on Ga–O distances. Figure 2 shows the final fit obtained between calculated and observed patterns and corresponds to a satisfactory crystal structure model indicator and profile factor (see Table 1).

**Solid-State NMR.** Solid-state NMR experiments were performed at 11.7 T on an Avance Bruker spectrometer equipped with a 2.5 mm double-tuned probe. A suite of one-dimensional (1D) and two-dimensional (2D) NMR was used, including 1D magic-angle spinning (MAS) <sup>1</sup>H, 2D MAS <sup>1</sup>H–<sup>1</sup>H double quantum to single quantum correlation (DQ), 2D MAS <sup>1</sup>H–<sup>1</sup>H radio-frequency-driven recoupling (RFDR), and 1D <sup>13</sup>C{<sup>1</sup>H} cross polarization (CP) MAS NMR. In <sup>1</sup>H MAS experiments, the relaxation delay between accumulations was 4 s, as the typical *T*<sub>1</sub> values measured in our samples by using the saturation method were smaller than 0.3 s. In the 2D experiments, the acquisition delay was reduced to 1 s. The sample rotation rate was 30 kHz for <sup>1</sup>H NMR experiments and 12.5

**Figure 2.** Final Rietveld plot of the activated MIL-68 (Ga) phase. A zoomed-in plot is shown in the inset.

kHz for <sup>13</sup>C{<sup>1</sup>H} CPMAS. The magnitude of the radio frequency field ( $\nu_{RF}$ ) in all <sup>1</sup>H NMR experiments was 33 kHz. In <sup>1</sup>H–<sup>13</sup>C CP, the  $\nu_{RF}$  (<sup>13</sup>C),  $\nu$  (<sup>1</sup>H) during CP, and  $\nu_{RF}$  (<sup>1</sup>H) during XiX decoupling values were 67.9, 55.4, and 66, respectively. The number of scans (NS) was 80 and 16 000 for 1D <sup>1</sup>H MAS and <sup>1</sup>H–<sup>13</sup>C CP, respectively. In <sup>1</sup>H–<sup>1</sup>H DQ MAS, the back-to-back (BABA) sequence was selected for excitation and reconversion of DQ coherences.<sup>37</sup> Using a rotor-synchronized *t*<sub>1</sub> increment of 33.3 μs and NS = 32 for a BABA pulse train length of 133 μs long, the acquisition times of 2D data were ca. 1 h. The RFDR experiments were acquired with NS = 8, *t*<sub>1</sub> increment = 66.6 μs, and mixing times  $\tau_m$  = 2.66 ms, leading to a total acquisition time of a 2D spectrum of ca. 2 h. One 180° pulse per rotor period was introduced during the mixing time.<sup>38</sup> All <sup>1</sup>H and <sup>13</sup>C chemical shifts are reported using the  $\delta$  scale and are referenced to tetramethylsilane at 0 ppm.

**Hydrogen Sorption Measurements.** Pressure-composition-isotherm curves for hydrogen sorption were performed at 77 K using a volumetric device (Sievert's method) equipped with calibrated and thermalized volumes and pressure gauges. The sample holder is a stainless steel container closed with a metal seal. The volumetric device with gauged volumes was immersed in a temperature-controlled water bath at 298 K, and high-purity hydrogen (Alphagaz H22, 6N) was introduced step by step up to 10 MPa. The sample holder connected to the volumetric device was immersed in liquid nitrogen, and the pressure variations due to both gas cooling and hydrogen adsorption were measured. The equation of state for hydrogen was obtained from the program GASPAC V3.32 (Cryodata, Inc.). All samples were measured twice (i.e., two full adsorption/desorption cycles) to check for hysteresis and reproducibility.

Before sorption measurements, the samples were outgassed under a primary vacuum (5 Pa) at 150 and 80 °C for MIL-68 (In and Ga) and MIL-110 (Al), respectively. Sample volume corrections were derived from density measurements obtained with a Helium Accupyc 1330 pycnometer on 100 mg of sample.

## Results

**Structure Description.** The structures of the gallium and indium terephthalates correspond to the topology previously

(37) Feike, M.; Demco, D. E.; Graf, R.; Gottwald, J.; Hafner, S.; Spiess, H. W. *J. Magn. Reson., Ser. A* **1996**, *122*, 214–221.

(38) Bennett, A. E.; Ok, J. H.; Griffin, R. G.; Vega, S. *J. Chem. Phys.* **1992**, *96*, 8624–8627.

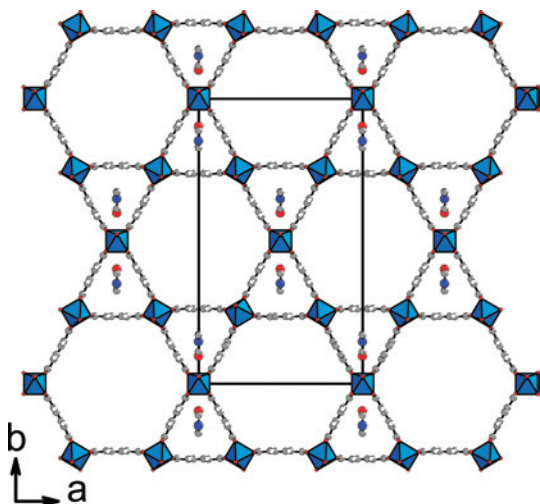


**Figure 3.** View of the structure of MIL-68 along the *c* axis, showing the arrangement of the hexagonal and triangular channels, with the Kagomé lattice type (3.6.3.6). N,N-dimethylformamide moieties are located in the triangular tunnels (from the MIL-68 (In) single-crystal analysis).

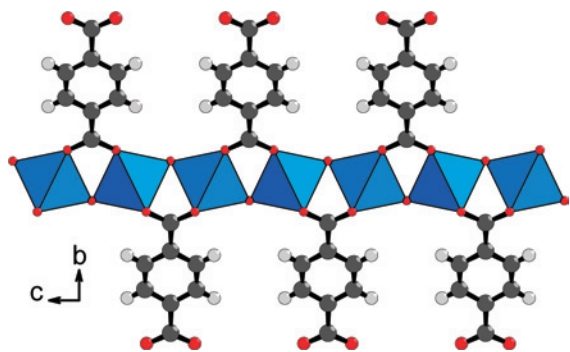


**Figure 4.** View of a chain of  $\text{MO}_4(\text{OH})_2$  octahedra in MIL-68 ( $M = \text{Ga}$  or  $\text{In}$ ). The octahedral units are trans-connected through the hydroxyl groups to form infinite files running along the *c* axis. Adjacent octahedra are linked to each other via the terephthalate ligands.

described in the vanadium-based compound MIL-68.<sup>31</sup> They are built up from infinite straight chains of metal-centered octahedra,  $\text{MO}_4(\text{OH})_2$  ( $M = \text{Ga}$  or  $\text{In}$ ), connected to each other through the terephthalate ligands (Figure 3). The octahedral units are linked together via two hydroxyl groups located in trans positions, and two adjacent octahedra are also connected via the carboxylate functions, which induce tilted chains (Figure 4). Such a one-dimensional inorganic motif was encountered in other metal-organic frameworks such as the solids MIL-53 and MIL-61, with gallium<sup>12,34,35</sup> and indium,<sup>18,21,27</sup> respectively. Other examples are also found in other porous compounds involving trivalent metals such as vanadium,<sup>29,39</sup> chromium,<sup>30,40</sup> iron,<sup>41–43</sup> or aluminum.<sup>8,9</sup> If the octahedra are considered as nodes, their connections with the terephthalate moieties give rise to the

formation of the so-called Kagomé<sup>32</sup> net (Schläfli notation 3.6.3.6), composed of hexagonal rings delimited by six triangular rings. The archetype Kagomé topology was primarily reported in purely inorganic networks such as the hexagonal bronze structure type found in the potassium tungstate  $\text{K}_x\text{WO}_3$ <sup>44</sup> or iron sulfates of the jarosite type.<sup>45,46</sup> The latter lattices are built up from the connection of corner-sharing octahedral species,  $\text{MO}_6$ , forming a network of three- and six-membered windows. This topology has been intensively studied for the solids incorporating magnetic metals, and in some cases, unusual magnetic properties with spin frustration behavior were observed.<sup>33</sup> Therefore, the MIL-68 network may be considered as an extension of the hexagonal bronze type with columns of octahedra,  $\text{MO}_4(\text{OH})_2$ , linked through the terephthalate ligands. It results in the generation of two types of channels with diameter openings of 6.0–6.4 and 16–17 Å for the triangular and hexagonal rings, respectively (estimated from calculations based on the ionic radius of 1.35 Å for oxygen). Besides the vanadium terephthalate MIL-68,<sup>31</sup> such a Kagomé lattice has already been reported in other coordination polymers with layerlike structures<sup>47–52</sup> or three-dimensional networks.<sup>53–55</sup>

In MIL-68, there exist two crystallographically inequivalent metallic sites (M1 and M2) located on the special positions  $1/4\ 1/4\ 1/2$  (8d) and  $0\ 0\ 1/2$  (4a), associated with the *trans*-hydroxyl groups in the positions  $x\ y\ 3/4$  (8g) for O1 and  $0\ y\ 3/4$  (4c) for O5. The valence bond calculations<sup>56</sup> give values of 1.11 (Ga) or 1.16 (In) for O1 (Ga) and 1.16 (Ga) or 1.44 (In) for O5, in good agreement with the occurrence of hydroxyl groups bridging the metallic atoms. The metal–oxygen distances found for MIL-68 are typical for trivalent metals with octahedral coordination: Ga–O distances range from 1.93 (apical) to 1.95 Å (equatorial) and In–O distances range from 2.024(1) (apical) to 2.152(1) Å (equatorial).

The single-crystal analysis of the indium compound allowed for the location of trapped species within the channels. In fact, N,N-dimethylformamide molecules were observed in the triangular tunnels (Figure 3) with strong hydrogen interactions between the oxygen atom of the formamide function and the hydroxyl groups bridging the

- (39) Barthelet, K.; Marrot, J.; Riou, D.; Férey, G. *Angew. Chem., Int. Ed.* **2002**, *41*, 281.  
 (40) Serre, C.; Millange, F.; Devic, T.; Audebrand, N.; Van Beek, W. *Mater. Res. Bull.* **2006**, *41*, 1550.  
 (41) Chu, D.-Q.; Pan, C.-L.; Wang, L.-M.; Xu, J.-Q. *Mendeleev Commun.* **2002**, 207.  
 (42) Whitfield, T. R.; Wang, X.; Liu, L.; Jacobson, A. J. *Solid State Sci.* **2005**, *7*, 1096.  
 (43) Sanselme, M.; Grenèche, J.-M.; Riou-Cavellec, M.; Férey, G. *Solid State Sci.* **2004**, *6*, 853.

- (44) Magnéli, A. *Acta Chem. Scand.* **1953**, *7*, 315.  
 (45) Greedan, J. E. *J. Mater. Chem.* **2001**, *11*, 37.  
 (46) Paul, G.; Choudhury, A.; Rao, C. N. R. *Chem. Commun.* **2002**, 1904.  
 (47) Moulton, B.; Lu, J.; Hajndl, R.; Hariharan, S.; Zaworotko, M. J. *Angew. Chem., Int. Ed.* **2002**, *41*, 2821.  
 (48) Perry, J. J.; McManus, G. J.; Zaworotko, M. J. *Chem. Commun.* **2004**, 2534.  
 (49) Liu, Y.; Kravtsov, V. C.; Beauchamp, D. A.; Eubank, J. F.; Eddaoudi, M. J. *Am. Chem. Soc.* **2005**, *127*, 7266.  
 (50) Wang, X.-Y.; Wang, L.; Wang, Z.-M.; Gao, S. *J. Am. Chem. Soc.* **2005**, *128*, 674.  
 (51) Eddaoudi, M.; Kim, J.; Vodak, D.; Sudik, A.; Wachter, J.; O'Keeffe, M.; Yaghi, O. M. *Proc. Natl. Acad. Sci. U. S. A.* **2002**, *99*, 4900.  
 (52) Nytko, E. A.; Helton, J. S.; Müller, P.; Nocera, D. G. *J. Am. Chem. Soc.* **2008**, *130*, 2922.  
 (53) Rusanov, E. B.; Ponomarova, V. V.; Komarchuk, V. V.; Stoeckli-Evans, H.; Fernandez-Ibanez, E.; Stoeckli, F.; Sieler, J.; Domasevitch, V. *Angew. Chem., Int. Ed.* **2003**, *42*, 2499.  
 (54) Chun, H.; Moon, J. *Inorg. Chem.* **2007**, *46*, 4371.  
 (55) Mahata, P.; Sen, D.; Natarajan, S. *Chem. Commun.* **2008**, 1278.  
 (56) Brese, N. E.; O'Keeffe, M. *Acta Crystallogr., Sect. B* **1991**, *47*, 192.

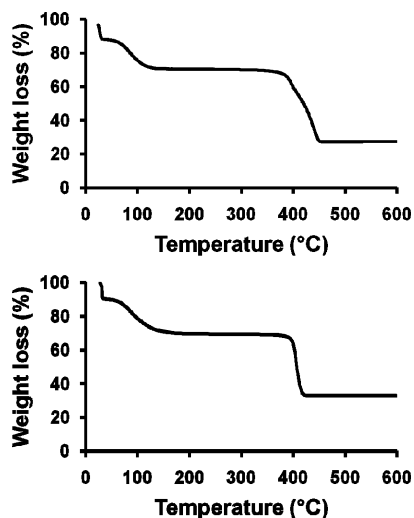


**Figure 5.** TG curves of the as-synthesized compounds (top) MIL-68 (Ga) and (bottom) MIL-68 (In) under an oxygen atmosphere ( $1\text{ }^{\circ}\text{C min}^{-1}$ ).

indium metals ( $\text{NHC}=\text{O}\cdots\text{HO} = 2.767(8)\text{ \AA}$ ). The DMF species are statistically disordered on two positions within the smaller channels. The Fourier map analyses did not reveal any other DMF, terephthalate, or water moieties trapped in the larger hexagonal channels. This is probably due to high disorder, whereas NMR experiments (see hereafter) show the presence of DMF in the hexagonal channels.

**Thermal Behavior.** The thermogravimetric analyses of both solids MIL-68 (Ga) and MIL-68 (In) have been carried out on a TA Instrument type 2050 apparatus with a heating rate of  $1\text{ }^{\circ}\text{C min}^{-1}$  under an oxygen flow. The thermogravimetric (TG) curves show similar weight loss behaviors for both compounds with three successive events (Figure 5). A first weight loss is assigned to the departure of trapped water from room temperature up to  $50\text{ }^{\circ}\text{C}$  and corresponds to  $2.3\text{ H}_2\text{O}$  (for Ga-based MIL-68) and  $2.2\text{ H}_2\text{O}$  (for In-based MIL-68) per metal unit (12.0% and 9.5%, respectively). The second event between  $50$  and  $150\text{ }^{\circ}\text{C}$  is attributed to the removal of the trapped DMF species, which corresponds to  $0.8\text{ DMF}$  (for Ga-based MIL-68) and  $1.2\text{ DMF}$  (for In-based MIL-68) per metal unit (17.4% and 20.8%, respectively). The last weight loss occurs with the decomposition of the terephthalate ligand from  $340\text{ }^{\circ}\text{C}$  for MIL-68 (Ga) (obsd, 43.3%; calcd, 44.6%) and  $350\text{ }^{\circ}\text{C}$  for MIL-68 (In) (obsd, 36.6%; calcd, 36.4%). After the collapse of the structure, the products transform into dense metal oxides,  $\text{M}_2\text{O}_3$  (Ga or In). From the thermogravimetric experiments together with the elemental analyses, chemical formulas could be estimated as follows:  $\text{Ga}(\text{OH})(\text{O}_2\text{C}-\text{C}_6\text{H}_4-\text{CO}_2)\cdot x\text{DMF}\cdot 2.3\text{H}_2\text{O}$  ( $x = 0.8-0.9$ ) and  $\text{In}(\text{OH})(\text{O}_2\text{C}-\text{C}_6\text{H}_4-\text{CO}_2)\cdot x\text{DMF}\cdot 2.2\text{H}_2\text{O}$  ( $x = 1.0-1.2$ ). It should be noted that extra nonbonded terephthalate ligands, which could be trapped within the channels, are not found for these two compounds. This differs with the situation encountered in the vanadium-based MIL-68,<sup>31</sup> for which a significant amount of free terephthalate anions (0.15 bdc/metal), but less DMF species (0.33 DMF/metal), are observed. The framework thermal stability is also slightly higher than that of the vanadium compound ( $300\text{ }^{\circ}\text{C}$ ).

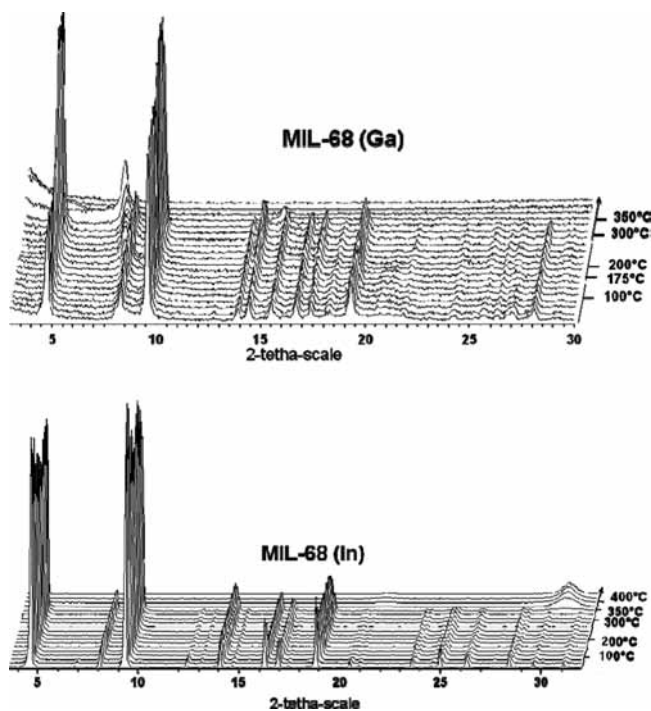


**Figure 6.** Thermodiffractograms of the as-synthesized compounds MIL-68 (Ga) and MIL-68 (In) under air using  $\text{Cu K}\alpha_{1,2}$  radiation.

Both Ga- and In-MIL-68 compounds have been analyzed by X-ray diffraction as a function of temperature under air. X-ray powder diagrams have been recorded with a Bruker AXS D5005 powder diffractometer using a diffracted-beam-graphite monochromator ( $\text{Cu K}\alpha_{1,2}$ ) equipped with an Anton Paar HTK1200 oven camera. Powder diffraction data were collected from room temperature up to  $450\text{ }^{\circ}\text{C}$  with a heating rate of  $22\text{ }^{\circ}\text{C h}^{-1}$  and over the angular range  $3-39^{\circ}$  ( $2\theta$ ) with a counting time of 4 s per step and a step length of  $0.04^{\circ}$  ( $2\theta$ ). The thermodiffractograms, represented in Figures 6, indicate no modification of the Bragg peaks up to  $\approx 350\text{ }^{\circ}\text{C}$  for the two phases. However, for MIL-68 (Ga), a second contribution appears at  $200\text{ }^{\circ}\text{C}$  with a broad diffraction peak at  $\approx 8.0^{\circ}$  ( $2\theta$ ), which is shifted toward a low angle ( $\approx 7.8^{\circ}$  ( $2\theta$ )) when the temperature increases. After the structure destruction, only this contribution is visible together with a second Bragg peak at  $15.4^{\circ}$  ( $2\theta$ ). This unidentified diffraction signature might reflect that the MIL-68 (Ga) network starts to undergo a slow phase transition from  $200$  to  $380\text{ }^{\circ}\text{C}$ , which induces the structure collapse. It should be noticed that this Bragg peak does not correspond to those of the other gallium terephthalate, MIL-53.<sup>35</sup> No such behavior is observed for the parent indium phase, and only the formation of nanocrystalline  $\text{In}_2\text{O}_3$  (PDF file 06-0416) is visible at  $350\text{ }^{\circ}\text{C}$ , with broad diffraction peak at  $30.5^{\circ}$  ( $2\theta$ ).

**NMR Spectroscopy.** Solid-state NMR results of the as-synthesized gallium-based MIL-68 compound are reported as follows. The  $^1\text{H}$  NMR spectrum and its decomposition by simulation are displayed in Figure 7. The two resolved signals at  $\delta = 0.8$  and  $1.2\text{ ppm}$  are assigned to the inequivalent hydroxyl groups of the gallium chains of the framework. The presence of mobile DMF is confirmed by the two sharp peaks at  $7.2$  and ca.  $2\text{ ppm}$ , in a relative proportion of 1:6. The ca.  $2.0\text{ ppm}$  peak is actually composed of two hardly resolved



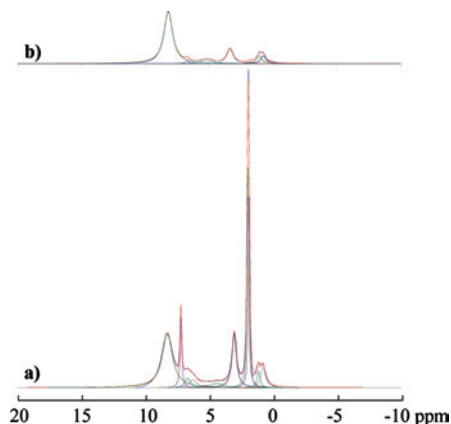


**Figure 7.** Experimental  $^1\text{H}$  MAS NMR spectra and simulated spectra with the decomposition of the as-synthesized (a) and rehydrated (b) MIL-68 (Ga).

signals, which correspond to the two methyl groups of DMF. The peak at 8.3 ppm is attributed to aromatic protons of framework terephthalate. At about 6.5 ppm, a broader component with some partial resolution is observed. This signal is assigned to a second type of crystallographically inequivalent terephthalate of the framework. A couple of signals, at 3.0 and ca. 4–5 ppm, are observed and assigned to water molecules, presumably in different local environments. On the basis of quantitative NMR, the following formula for MIL-68 (Ga) is proposed:  $\text{Ga}(\text{OH})(\text{O}_2\text{C}-\text{C}_6\text{H}_4-\text{CO}_2) \cdot x\text{DMF} \cdot y\text{H}_2\text{O}$ , with  $x = 0.7 \pm 0.1$  and  $y = 1.5 \pm 0.1$ , which is close to the elementary and thermogravimetric analyses.

The spectrum (Figure 7) of the rehydrated MIL-68 (Ga) compound was recorded from a sample calcined at 200 °C overnight and then placed in a rotor under ambient atmosphere. It exhibits the same feature observed in the parent materials, except signals of encapsulated DMF, which are detected as traces. This result indicates that DMF and water of the as-synthesized phase are present as guest molecules within the pores of the compound and can be extracted by calcination without the collapse of the structure. After ambient air exposure, MIL-68 (Ga) is able to adsorb water, as can be shown in the  $^1\text{H}$  spectrum (Figure 7b). The resonance peak at 3.4 ppm assigned to water is still visible. The chemical formula of the rehydrated compound determined by NMR is therefore as follows:  $\text{Ga}(\text{OH})(\text{O}_2\text{C}-\text{C}_6\text{H}_4-\text{CO}_2) \cdot y\text{H}_2\text{O}$  with  $y = 0.9 \pm 0.4$ . However, one may notice that a lower amount of water is observed in the rehydrated phase, although all of the DMF species have been removed.

The  $^{13}\text{C}\{^1\text{H}\}$  NMR spectrum of the as-synthesized MIL-68 (Ga) and its decomposition by simulation are displayed in Figure 8. Two pairs of signals at  $\delta = 28.4$  and 33.3, on one hand, and 30.2 and 35.5 ppm, on the other hand, are visible in the methyl chemical shift range, indicating the existence of two types of DMF within the structure. Accordingly, two distinct signals are present at 164.9 and 163.1 ppm due to the carbonyl functions of the two different DMF molecules. A substantial difference in their respective line widths can be easily observed, suggesting two distinct dynamic behaviors. These species are almost in approximately a 1:1 ratio. The presence of bdc moieties is confirmed by two groups of overlapping signals of aromatic carbons

in the chemical shift ranges of 130–132 and 137–139 ppm and by resonances of carboxylic functions appearing at 170.7, 171.0, 171.7, and 172.5 ppm. The spectrum of the rehydrated MIL-68 (Ga) sample is shown in Figure 8b. However, NMR signatures of bdc carbon resonances have also changed upon activation of the material. Indeed, the spectrum becomes less complex, showing a broad signal at 129.6 ppm (corresponding to aromatic carbons linked to hydrogen) and three narrow resonances of equal population at 136.7, 137.6, and 138.3 ppm (corresponding to aromatic carbon linked to the carboxylate groups) and two peaks at 171.3 and 171.9 ppm in a 2:1 ratio for carboxylate functions. This result is fully consistent with three crystallographically inequivalent sites of carboxylates, which are only partially resolved in the carboxylic chemical shift range, but well-resolved in the aromatic signals range of carbons bearing the carboxylic functions. This observation supports the assessment of the orthorhombic space group (*Cmcm*) chosen for the description of the MIL-68 network instead of the hexagonal one (*P6<sub>3</sub>/mmc*). In the latter symmetry, only one single crystallographic site is expected for the carboxylate groups, whereas three carboxylate groups do occur with a ratio of 1:1:1 in the orthorhombic system. As observed from XRD analysis, the shift from hexagonal toward orthorhombic symmetry is due to the positions of terephthalate ligands rather than those of the heavy metal atoms. The organic linkers are found to be slightly shifted from the ideal hexagonal geometry.

The  $^{13}\text{C}$  spectrum of the rehydrated sample confirms the departure of almost all DMF molecules from the structure. Only traces of one of the two DMF types are still present at resonances of 28.4, 33.1, and 164.3 ppm. This result supports the idea that two kinds of DMF are present, with different interactions with the framework. One kind has a higher mobility and is therefore more easily removed, whereas the second kind has stronger interactions with the inorganic network. This is well-correlated to the different locations of DMF molecules within the tunnels. From the single-crystal XRD analysis, the MIL-68 (In) structure shows that DMF species are clearly visible within the small triangular channels in strong hydrogen-bond interactions with hydroxyl groups, whereas other DMF species are assumed to be present in larger hexagonal channels with less geometrical constraints.

The comparison of the two  $^{13}\text{C}$  spectra with and without activation demonstrates that the activated framework is definitely better defined. For the as-synthesized compound, the presence of two types of DMF interacting with the framework makes the  $^{13}\text{C}$  spectrum a superposition of probably two types of local situations with an identical inorganic framework. The noticeable change of the aromatic CH carbon resonance at about 130 ppm, with multiple narrow lines for the as-synthesized compound and a unique broader line at 129 ppm for the activated sample, indicates that the interaction of DMF takes place with these CH sites. However, not all bdc linkers will undergo such a definite interaction, leading to the augmented multiplicity of the carbons lines in the as-synthesized compound versus the activated one.

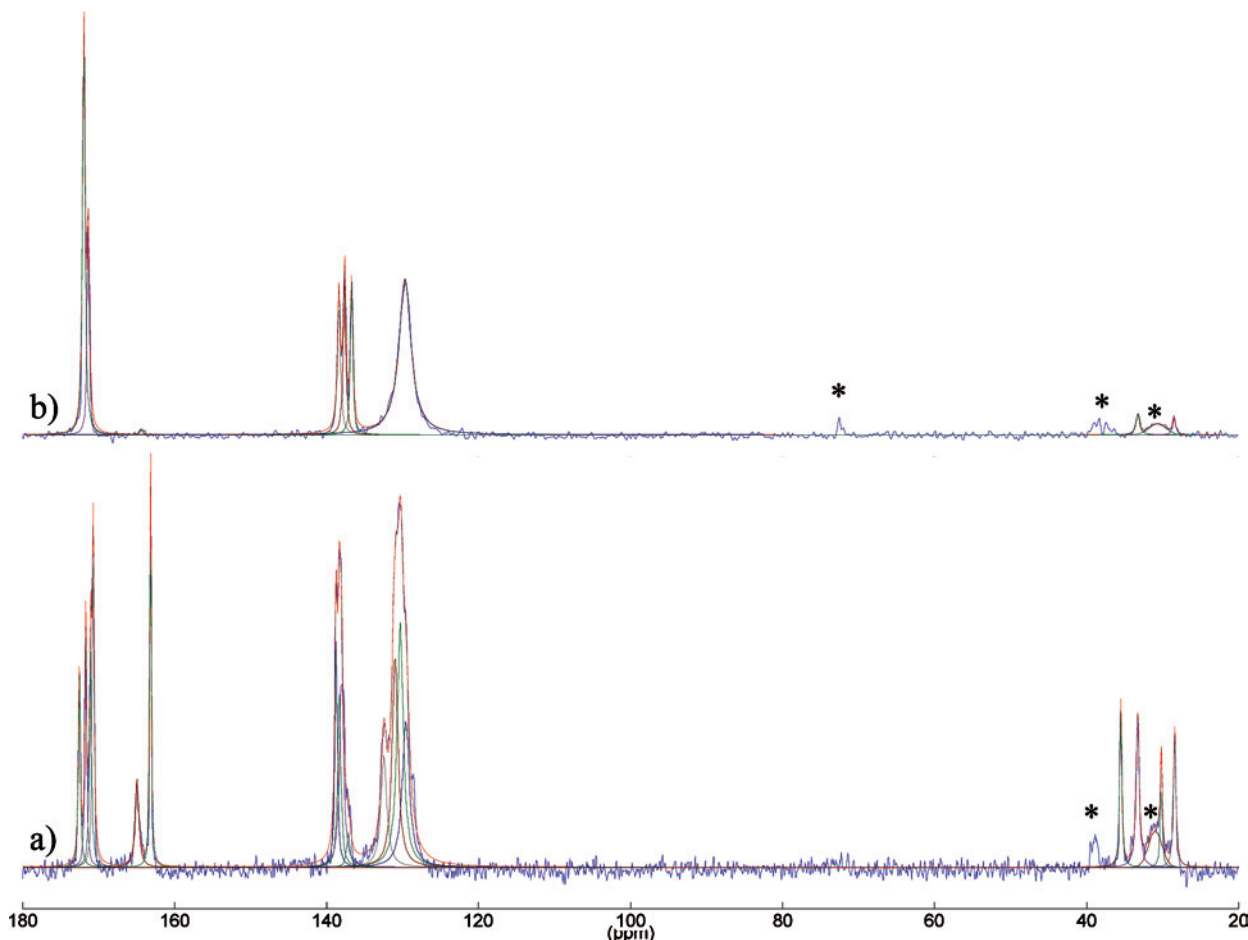


**Figure 8.** Experimental  $^{13}\text{C}\{^1\text{H}\}$  CPMAS NMR spectra and simulated spectra with the decomposition of the as-synthesized (a) and rehydrated (b) MIL-68 (Ga). An asterisk (\*) indicates spinning side bands.

In order to gain further details on the interactions between framework and extra-framework species within the materials, additional 2D homonuclear recoupling techniques,  $^1\text{H}-^1\text{H}$  DQ and  $^1\text{H}-^1\text{H}$  RFDR, have been applied on the as-synthesized sample. The  $^1\text{H}-^1\text{H}$  RFDR (Figure 9a) and  $^1\text{H}-^1\text{H}$  DQ (Figure 9b) experiments provide complementary information. The former maps zero-quantum to single-quantum correlations, while the latter maps double-quantum to single-quantum correlations. Moreover, the DQ experiment enables autocorrelations between identical crystallographic sites. The results of all correlations observed in RFDR and DQ experiments are summarized in Tables 2 and 3, respectively.

In the RDFR experiment, the DMF resonances ( $\text{CH}_3$  and CHO) are correlated, confirming their assignment. On the other hand, these protons are not correlated with any other protons, indicating that such molecules are somehow dipolarly decoupled, by motion or by the distance. The hydroxyl group resonances are correlated with the 8.3 as well as the 6.7 ppm signals, both being aromatic protons. The water signal at 3.0 ppm does not exhibit any cross peak, indicating a strong dipolar decoupling by motion.

In the DQ experiment, no DQ self-coherence is detected for the water at 3.0 ppm, indicating a weak dipolar interaction between them. Their motion in the inorganic frame is most probably the origin of such a vanishing dipolar interaction.

The signals at 3–4 ppm are therefore assigned to mobile water molecules filling the channels. Some very weak cross peaks are also observed between the bdc signal and water signals at 3–4 ppm. Strong self-correlations between the bdc signal at 8.3 ppm are present. Strong correlations between 8.3 ppm signals and 6.5 ppm signals can be observed. No self-correlation can be observed for the 6.5 ppm signals. As both 8.3 and 6.5 ppm signals are assigned to aromatic protons, it can be deduced that only intermolecular dipolar coupling correlations are observed. Such intermolecular correlations exist for the 8.5 ppm signals and not for the 6.5 ppm signals. One may infer that, in the as-synthesized compound, proximities between the 8.5 ppm bdc sites are present but not direct proximities between the 6.5 ppm sites, due to probable specific interactions with DMF. The confirmation of these two different bdc's comes from the rehydrated compound, for which only one type of bdc remains when the DMF is removed from the phase.

No extra-framework carboxylic acid signal can be seen in the proton spectra, confirming that the material is free of nonreacted organic ligands, contrary to the vanadium-based analog compound. Such extra-framework organic residue should occur at ca. 12.5 ppm for  $-\text{COOH}$  groups, as observed in the aluminum terephthalate  $\text{Al}(\text{OH})(\text{O}_2\text{C}-\text{C}_6\text{H}_4-\text{CO}_2)\cdot(\text{HO}_2\text{C}-\text{C}_6\text{H}_4-\text{CO}_2\text{H})_{0.7}$  (MIL-53).<sup>8</sup> The terephthalate signals showed correlations with all other signals except that



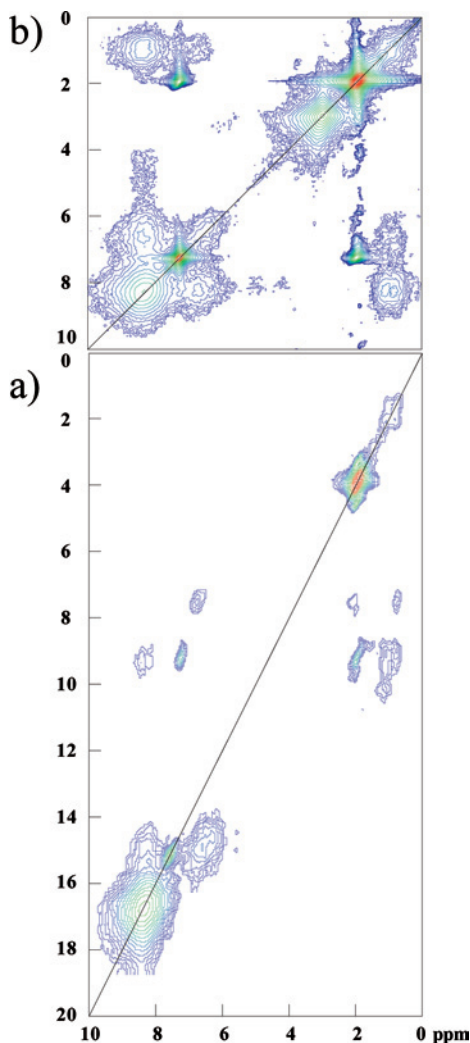


**Figure 9.**  $^1\text{H}$ – $^1\text{H}$  DQ (a) and  $^1\text{H}$ – $^1\text{H}$  RFDR (b) MAS NMR spectra of the as-synthesized MIL-68 (Ga).

**Table 2.** Correlations Observed in the  $^1\text{H}$ – $^1\text{H}$  RFDR Experiment on the As-Synthesized MIL-68 (Ga)

species	$\delta$ (ppm)	OH		DMF <sup>a</sup>			H <sub>2</sub> O		bdc		DMF <sup>b</sup>		bdc
		0.7	1.1	1.9	3.0	4.3	4.9	6.3	6.7	7.3	8.4		
OH	0.7												X
	1.1												X
DMF <sup>a</sup>	1.9											X	
H <sub>2</sub> O	3.0												
	4.3												X
	4.9												X
bdc	6.3												X
	6.7	X											X
DMF <sup>b</sup>	7.3			X									
bdc	8.4	X	X				X	X	X	X			

<sup>a</sup> CH<sub>3</sub> group in DMF. <sup>b</sup> CHO function in DMF.

of DMF, consistent with their spatial proximities with all other species. Actually, even if weak in the SQ MAS spectrum, a signal at 7.6 ppm appeared in the DQ experiment, which is assigned to one other DMF proton (–HCO), the main one being at 7.2 ppm. This is related to the two types of DMF observed in the <sup>13</sup>C spectrum.

**Measurement of the BET Surface Area.** Both activated MIL-68 (Ga) and MIL-68 (In) were tested for adsorption capacities with nitrogen. The porosity of both compounds was estimated by gas sorption isotherm experiments in liquid

**Table 3.** Correlations Observed in the  $^1\text{H}$ – $^1\text{H}$  DQ Experiment on the As-Synthesized MIL-68 (Ga)

Species <sup>a</sup>	$\delta$ (ppm)	OH		DMF <sup>a</sup>		bdc		DMF <sup>b</sup>		bdc	
		0.8	1.0	2.0	6.1	6.6	7.2	7.6	8.4		
OH	0.8	X					X				X
	1.0		X								X
DMF <sup>a</sup>	2.0			X				X			
bdc	6.1										X
	6.6	X									X
DMF <sup>b</sup>	7.2				X						
bdc	7.6										X
	8.4	X	X			X	X				X

<sup>a</sup> CH<sub>3</sub> group in DMF. <sup>b</sup> CHO function in DMF.

nitrogen using the Micromeritics ASAP2010 apparatus. Typical isotherms of type I are observed with a plateau at 320 cm<sup>3</sup>/g (STP) and 260 cm<sup>3</sup>/g (STP) on the activated samples (degassed at 150 °C overnight under a primary vacuum). From these data, the BET and Langmuir apparent surface areas were calculated as 1117(24) and 1410(2) m<sup>2</sup> g<sup>−1</sup> (micropore volume: 0.46 cm<sup>3</sup> g<sup>−1</sup>) for MIL-68 (Ga) and 746(31) and 1139(5) m<sup>2</sup> g<sup>−1</sup> (micropore volume: 0.44 cm<sup>3</sup> g<sup>−1</sup>) for MIL-68 (In), respectively. These surface areas are much larger than the values reported in the vanadium<sup>31</sup> MIL-68 analog at 603(22) (BET) and 847(1) m<sup>2</sup> g<sup>−1</sup> (Langmuir). The surface areas are quite distinct for the MIL-68 phases incorporating different cations, but they are not correlated to their molecular weight differences. If MIL-68 (Ga) is taken as a reference, there would be a variation of +18% (mol wt) for the indium form and −7.5% (mol wt) for the vanadium one. This would lead to the expected BET values of 1200 m<sup>2</sup> g<sup>−1</sup> with vanadium and 916 m<sup>2</sup> g<sup>−1</sup> with indium. Moreover, a recent computer simulation study<sup>57</sup> reported that the theoretical accessible surface area was calculated as 3333 m<sup>2</sup> g<sup>−1</sup> for MIL-68 (V). Our experimental values are quite far from that reported by Düren et al.,<sup>57</sup> and these observations might reflect some issues concerning the activation process in order to get the empty pore solids in the metal-organic framework materials. However, in the case of the MIL-68 phases, many attempts were carried out in order to find a suitable activation process without collapsing the hybrid network, and the calcination procedure (150 °C under a vacuum overnight) was found to be the best for obtaining the empty pore phase. Moreover, the NMR analysis of the MIL-68 (Ga) clearly confirmed this assessment, showing the departure of almost all encapsulated organic species from the pore channels upon activation. We may say that the measured surface areas using the BET method would give relative evidence concerning the state of porosity of the MIL-68 phases, for which careful structural characterization did not lead to converging values between calculation and experimental results. This series of observations also pointed out the difficulty for obtaining maximum accessible porosity in some MOF materials.

**Hydrogen Sorption.** The hydrogen adsorption capacity was measured for both MIL-68 samples following the previously described activation (150 °C under a vacuum overnight). Weight losses were found to be in agreement

(57) Düren, T.; Millange, F.; Férey, G.; Walton, K. S.; Snurr, R. Q. *J. Phys. Chem. C* **2007**, *111*, 15350.

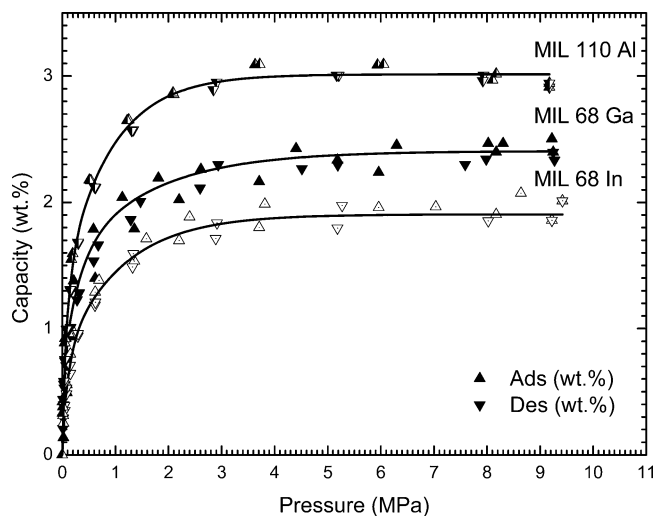


**Figure 10.** Hydrogen adsorption isotherms at 77 K of the metal terephthalate MIL-68 (Ga), MIL-68 (In), and aluminum trimesate MIL-110.

with those reported in the above thermal behavior section. For comparison, a sample of the aluminum trimesate MIL-110,<sup>11</sup> whose framework also exhibits one-dimensional channels with a 16 Å aperture diameter, was tested.

The hydrogen uptakes at 77 K show a very fast adsorption process for Ga, whereas a slower behavior was observed for the In compound. It is worth noting that the same trend was also observed for the BET measurements with N<sub>2</sub> adsorption, confirming that this behavior is intrinsic to the samples. Nevertheless, both phases exhibit type-I curves or Langmuir isotherm profiles, as expected for physisorption. The MIL-68 (Ga and In) compounds reversibly adsorb up to 2.46 wt % and 1.98 wt % of hydrogen, respectively, at 77 K under a saturated pressure of 4 MPa. Isotherm curves are fully reversible and do not show hysteresis effects. Measurements were reproducible for both cycles, as shown in Figure 10. The capacity reported for MIL-68 (In) is significantly lower than that of Ga but in good agreement with the molar mass increase and the surface area decrease induced by the replacement of heavier In atoms by Ga ones. Therefore, the amount of active sites for adsorption is expected to be the same for both compounds. It shows however that the nature of the metal center does not play a key role here in the sorption process and that hydrogen uptake is mainly governed by textural parameters. Similarly, the aluminum trimesate MIL-110 exhibits a hydrogen uptake of 3 wt %, a value larger than that of the two former ones, confirming the key role played by the molar mass of the metal building units.

It is noteworthy that the hydrogen uptakes reported here are smaller than those previously reported for the aluminum (or chromium) terephthalate MIL-53<sup>58</sup> (3.8 wt % under 1.6 MPa) or the extra-large pore compounds MIL-100/MIL-101<sup>59</sup> (3–6 wt %) or MOF-177<sup>60</sup> (up to 7.5 wt % under 7

MPa). For the latter cases, this can be understood if one compares the limited surface area of the present compounds (1100–1400 m<sup>2</sup> g<sup>-1</sup>) to the huge ones of three-dimensional MIL-101 (5900 m<sup>2</sup> g<sup>-1</sup>) or MOF-177 (5640 m<sup>2</sup> g<sup>-1</sup>). Again, a strong correlation exists between texture and gas sorption, and it is probably more worthy to compare MIL-68 with MIL-53, as both compounds exhibit 1D channel structures and comparable surface areas (1500 m<sup>2</sup> g<sup>-1</sup> for MIL-53).

## Conclusion

This study describes the synthesis route for the preparation of the gallium and indium terephthalate MIL-68 analogs, which were previously reported with vanadium.<sup>31</sup> Their crystal structures consist of infinite chains of trans-connected metal-centered octahedra, MO<sub>4</sub>(OH)<sub>2</sub>, linked to each other through the terephthalate ligand. The resulting three-dimensional organic–inorganic network, determined by means of X-ray diffraction (single-crystal and powder), is based on a Kagomé lattice delimiting two different one-dimensional channels parallel to the inorganic chains. These two tunnels have triangular and hexagonal shapes, corresponding to aperture diameters of 6 and 16–17 Å, respectively. Although the cation arrangement is compatible with a hexagonal symmetry, the MIL-68 crystal structure is orthorhombic with a double cell volume, due to the positions of the organic linkers, which are slightly shifted from the ideal hexagonal symmetry. The solid-state NMR spectroscopy involving <sup>1</sup>H and <sup>13</sup>C clearly supports this structural feature since splitting resonance peaks for bridging hydroxyl groups (<sup>1</sup>H) and carboxylates (<sup>13</sup>C) are observed. Moreover, a procedure of evacuation of the trapped species (H<sub>2</sub>O and DMF) within the channels was analyzed by NMR, and it has been shown that an empty pore solid could be obtained after heating the sample at 150 °C under a primary vacuum. BET surface areas were measured to be 1117(24) and 746(31) m<sup>2</sup> g<sup>-1</sup> for the gallium and indium forms, respectively. These compounds were able to sorb hydrogen with 2.46 and 1.98 wt % uptakes at liquid-nitrogen temperatures. Such sorption properties are in good agreement with the textural parameters reported for this family of compounds.

As this Kagomé-like topology occurs with V, Ga, and In, current studies are devoted to the synthesis of the MIL-68 analogs containing other trivalent metals like aluminum or iron cations.

**Acknowledgment.** The authors are grateful to thank Dr. Eric Leroy (ICMPE-CMTR, Thiais) for his help in the collection of the SEM images and indebted to the French ANR-PANH project “MATHYSSE” for financial support.

**Supporting Information Available:** CIF files and a PDF file containing additional tables. This material is available free of charge via the Internet at <http://pubs.acs.org>.

IC801624V

(58) Férey, G.; Latroche, M.; Serre, C.; Millange, F.; Loiseau, T.; Percheron-Guégan, A. *Chem. Commun.* **2003**, 2976.

(59) Latroche, M.; Surblé, S.; Serre, C.; Mellot-Draznieks, C.; Llewellyn, P. L.; Lee, J.-H.; Chang, J.-S.; Jung, S. H.; Férey, G. *Angew. Chem., Int. Ed.* **2006**, *45*, 8227.

(60) Wong-Foy, A. G.; Matzger, A. J.; Yaghi, O. M. *J. Am. Chem. Soc.* **2006**, *128*, 3494.